Revue des Energies Renouvelables Vol. 10 N°3 (2007) 367 – 379

Numerical modelling of combined heat and mass transfer in a tubular adsorber of a solid adsorption solar refrigerator

W. Chekirou*, N. Boukheit and T. Kerbache

Department of physics, University of Mentouri, Constantine 25000, Algeria

(reçu le 29 Octobre 2006 – accepté le 25 Septembre 2007)

Abstract - *In this paper a theoretical model of the heat and mass processes in a tubular adsorber of a solid adsorption solar refrigerator is established. The modelling and the analysis of the adsorber is the key of such studies because of the complex coupled heat and mass transfer phenomena that occur during the working refrigeration cycle. This model consists of the energy equation in the adsorbent layers, the energy balance equation of the adsorber wall, and state equation of the bivariant solid-vapour equilibrium using the Dubinin-Astakhov model to describe the phenomena of adsorption with the pair activated carbon AC-35/ methanol as an adsorbent/adsorbate. The influence of the main parameters on the system is also discussed.*

Résumé - *Dans cet article, un modèle théorique de simulation a été établi pour décrire l'échange de chaleur et de masse dans un adsorbeur tubulaire d'un réfrigérateur solaire à adsorption solide. La modélisation et l'analyse de l'adsorbeur est une étape essentielle dans cette étude en raison des phénomènes complexes de transfert de masse et chaleur qui se produisent lors du cycle de réfrigération. Ce modèle est basé sur la mise en équation d'énergie dans les couches d'adsorbant, ainsi que l'équation du bilan énergétique de la paroi de l'adsorbeur et l'équation de l'état d'équilibre bivariant solide-vapeur en utilisant le modèle de Dubinin-Astakhov pour décrire le phénomène d'adsorption du couple charbon actif AC-35 /méthanol comme adsorbant/adsorbat. Ce modèle nous permet de prévoir l'influence des paramètres principaux sur le système de réfrigération.*

Key words: Solar refrigerator - Adsorption - Heat and mass transfer - Activated carbon AC-35 / methanol - Solar performance coefficient.

1. INTRODUCTION

Ecological problems and energy crisis over the world have motivated scientists to develop energy systems more sustainable, having as one of the possible alternative the use of solar energy as source for cooling systems. In the field of the sorption cooling, there are three kind of system: liquid absorption, solid absorption (chemical reaction) and adsorption. In all these systems, the mechanical energy consumption is kept to a minimum or null. They can operate with low-grade heat from different sources such as waste heat or solar energy. The great advantage of adsorption systems over absorption ones is that they can operate without moving parts, having then lower costs of maintenance. Other advantages in comparison with the compression systems are: simple construction, environmentally benign and noiseless. A lot of applications for adsorption cooling systems have been viewed in both developed and developing countries such as: storage and conservation of vaccine, medical products, food conservation (vegetable, meat, fish,…), refrigeration, air conditioning, chillers and ice production.

The performance analysis of solar adsorption systems has been carried out by many researchers by several methods [1-5], and a great number of refrigerators have been built and tested [6-17] in the last two decades. The difference among the main developed models generally lies in the simplifying assumptions, the numerical resolution method, design and the use of a given system, and all these results show that the optimization of the refrigeration system is necessary before any practical application.

The objective of this work is to analyse the heat and mass transfer process in a tubular adsorber, this last is the most important components of such systems. So, a mathematical model

* chekirouw@yahoo.fr

based on uniform pressure and non uniform temperature distribution inside it has been developed in order to determine the influence of operating conditions on the system such as: condensation temperature, evaporation temperature, adsorption temperature, total solar energy absorbed by the collector and the collector configuration.

2. ANALYSIS OF THE ADSORPTION CYCLE

2.1 Principle of adsorption

Adsorption constitutes a solid sorption process by which the binding forces between fluid molecules (adsorbate) and the solid medium (adsorbent) derive from an electrostatic origin or from dispersion-repulsion forces. It is an exothermic and reversible process as a result of the gas-liquid phase change without modification of the solid it self. The adsorbed mass is obtained from the state equation of the bivariant solid-vapour equilibrium using Dubinin-Astakhov model, given by the following expression [1]:

$$m = w_0 \, \rho_l(T) \exp\left[- D \left(T \ln \frac{P_s(T)}{P} \right)^n \right] \tag{1}$$

The liberated energy during the adsorption is called isosteric heat of adsorption and its intensity depends on the nature of the adsorbent/adsorbate pair, the adsorbed mass and the latent heat L, it is given by the following equation [18]:

$$q_{st} = L(T) + R\,T \ln\left(\frac{P_s(T)}{P} \right) + \left[\frac{\alpha R T}{n D} \right] \left[T \ln \frac{p_s}{P} \right]^{(1-n)} \tag{2}$$

2.2 Cycle description

The figure 1 represent a schematic of an intermittent solar adsorption cooling system is It consists of a copper adsorber (or a solar reactor) containing the adsorbent, which depends on the temperature and the pressure; it can be isolated and connected to the condenser or to the evaporator by a non-return valves.

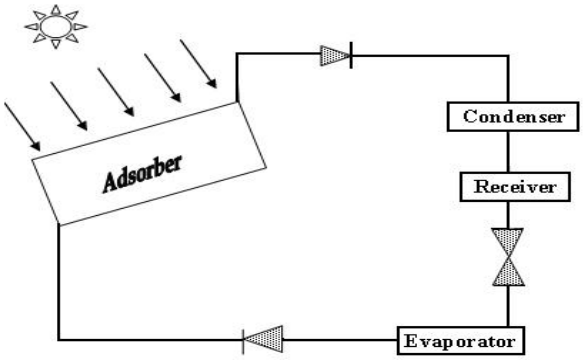

Fig. 1: Schematic diagram of simple solar adsorption refrigerator

Theoretically, the cycle consists of two isosters and two isobars, as illustrated in the Clapeyron diagram (Fig. 2). The process starts at point 1, where the adsorbent is at a low temperature T_a (adsorption temperature) and at low pressure P_e (evaporation pressure). While the adsorbent is heated by a solar energy, the temperature and the pressure increase along the isoster which the mass of the adsorbate in the adsorbent remains constant at m_{max}. The adsorber still isolated until the pressure reaches the condenser pressure, point 2 (the limit point of

desorption T_{c1}). At this time, the adsorber is connected with the condenser and the progressive heating of the adsorbent from point 2 to 3 causes a desorption of methanol and its vapour is condensed in the condenser and collected in a receiver. When the adsorbent reached its maximum temperature value T_g (regenerating temperature) and the adsorbed mass decreases to its minimum value m_{min} (point 3), the adsorbent starts cooling along the isoster at a constant mass m_{min} to point 4 (the limit point of adsorption T_{c2}). During this isosteric cooling phase, the adsorbent pressure decrease until it reaches the evaporator pressure P_e . After that, the adsorber is connected to the evaporator, and both adsorption and evaporation occur while the adsorbent is cooled from point 4 to 1. In this phase, the adsorbed mass increases up to its maximum m_{max} at point 1. The adsorbent is cooled until the adsorption temperature T_a by rejecting the sensible heat and the heat of adsorption. During this phase the cold is produced.

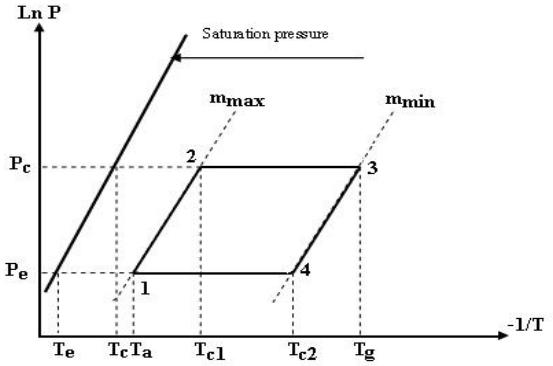

Fig. 2: Clapeyron diagram (lnP vs -1/T) of ideal solid adsorption cycle

3. MATHEMATICAL MODEL

The solar reactor studied in this work is shown in figure 3; the rear and the lateral insulation are used to limit the thermal losses; the activated carbon AC-35 is packed in the annular space between two coaxial tubes (Fig. 3); the inner tube is perforated to ease methanol flow to and from the activated carbon. A number of such tubes is linked to common methanol inlet and outlet headers (Fig. 4).

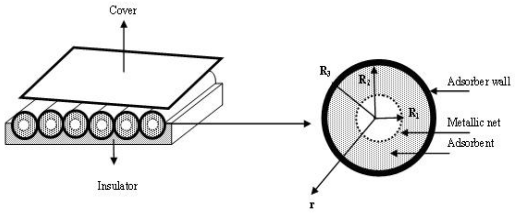

Fig. 3: Scheme of the solar reactor geometry

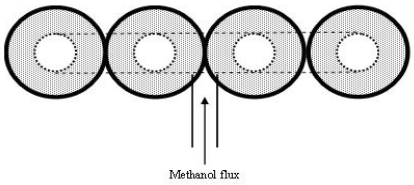

Fig. 4: Schematic of the link tubes of the adsorber

In order to analyse the evolution of the heat and mass transfer process in the adsorbent bed, which is the heart of the system, and to identify the parameters that influence the system performance, a simplified mathematical model has been developed using the following assumptions:

- The thermodynamic equilibrium of the adsorbent / adsorbate system in all point of the adsorber and any given moment;
- Diffusion occurs only in the gaseous phase;
- The resistance to mass diffusion though the interparticle voids and the pore is neglected;
- The adsorbate – adsorbent system is treated as a continuous medium for the thermal conduction effect;
- The pressure is assumed to be uniform in the reactor (grad p = 0);
- Side effects in the solar reactor casing are neglected;
- The system is considered to be one-dimensional, so, the adsorbent temperature is a function only of the radial direction;
- The convection effects within the porous bed are negligible;
- The wall adsorber is homogeneous, thus the thermo physical properties of them will be the same at all points;
- The specific heat of the adsorbed methanol is equal to that of the bulk liquid methanol;
- In the phase adsorption - evaporation and desorption - condensation the vapor pressure equals the saturation pressure at the evaporation and condensation temperature, respectively.

3.1 Energy equation

Under the above assumptions, the adsorbent bed energy equation can be expressed as follow [18]:

$$\rho_2\left(C_{p2} + mC_{pl}\right)\frac{\partial T}{\partial t} = k\left(\frac{\partial^2 T}{\partial r^2} + \frac{1}{r}\frac{\partial T}{\partial r}\right) + \rho_2 q_{st}\frac{\partial m}{\partial t} \tag{3}$$

The substitution of the differentiation of the equation (1) in the equation (3), gives the final energy equation of heat and mass transfer in the adsorbent bed:

$$\rho_2\left(C_{p2} + mC_{pl} + \frac{bq_{st}^2}{RT^2}\right)\frac{\partial T}{\partial t} = k\left(\frac{\partial^2 T}{\partial r^2} + \frac{1}{r}\frac{\partial T}{\partial r}\right) + \rho_2 q_{st} b\frac{\partial \ln p}{\partial t} \tag{4}$$

Where: $b = n D m T^n \left(\ln\frac{p_s(T)}{p}\right)^{n-1}$

3.2 Initial and boundary conditions

At the beginning of the cycle the temperature distribution of the adsorbent bed and adsorber wall can be considered as uniform and equal to the ambient temperature at the sunrise and the pressure equal to the evaporator pressure:

$$\begin{aligned} &T(r, t=0) = T_w(t=0) = T_{amb} \\ &p(t=0) = p_e = p_s(T_e) \\ &m = m(T_{amb,}\ p_e) \end{aligned} \tag{5}$$

The exact knowledge of the boundary conditions is necessary to the solution of the system's equation (1-5) during heating and cooling periods of solar solid adsorption cycle.

The geometry of the adsorber is cylindrical, therefore, the boundary condition is a symmetry condition expressed by the following equation at the interface ($r = R_1$):

$$\left.\frac{\partial T}{\partial r}\right|_{\gamma=R_1} = 0 \tag{6}$$

At the interface adsorbent bed – adsorber wall ($r = R_2$), there is a heat exchange characterized by a heat transfer coefficient h, this condition translated into:

$$h\left(T_w - T_{r=R_2}\right) = k\left.\frac{\partial T}{\partial r}\right|_{r=R_2} \tag{7}$$

where: T_w is the metallic wall temperature of the adsorber (the temperature at the interface $r = R_3$), that is given by the energy boundary condition and by the application of the heat balance between the adsorber wall (of length L_t and both external and internal diameter D_3 and D_2, respectively) and the ambiance; the following differential equation can be derived:

$$C_w \rho_w V_w \frac{\partial T_w}{\partial t} = \tau_v \alpha_w G(t) D_3 L_t - U_L D_3 L_t \left(T_w - T_{amb}\right) - h \pi D_2 L_t \left(T_w - T_{r=R_2}\right) \tag{8}$$

The overall heat losses coefficient U_L is given by:

$$U_L = U_{top} + U_{bot} + U_{side} \tag{9}$$

U_{top}, U_{bot} and U_{side} are respectively, the heat losses coefficient at the top, the bottom and the sides of the adsorber, where the side losses coefficient are assumed negligible.

Three kinds of transparent cover are considered for the solar collector; a single glazing, double glazing and TIM cover (Transparent insulation material).

In the first case, Duffie and Beckman [19] give an empiric relation due to Klein allowing to calculate the top heat losses coefficient U_{top} for temperatures ranging between 0°and 200 °C with an error lower or equal to $\pm 0.3\,W/m^2\,K$:

$$U_{top} = \left[\frac{N_v}{\frac{c}{T_w}\left(\frac{T_w - T_{amb}}{N_v + f}\right)^e} + \frac{1}{h_V}\right]^{-1} + \frac{\sigma\left(T_w + T_{amb}\right)\left(T^2 + T_{amb}^2\right)}{\left(\varepsilon_w + 0.0059 N_v h_v\right)^{-1} + \frac{2N_v + f - 1 + 0.133\varepsilon_w}{\varepsilon_g} - N_v} \tag{10}$$

Where

$$f = \left(1 + 0.089\, h_v - 0.1166\, h_v\, \varepsilon_w\right)\left(1 + 0.07866\, N_v\right)$$

$$e = 0.43\left(1 - 100/T_w\right)$$

$$h_v = 2.8 + 3\,V$$

$$c = 520\left(1 - 0.000051\,\beta^2\right) \quad \text{for} \quad 0° \prec \beta \prec 70°$$

where: β is the collector inclination, which is assumed equal to 37.3° for Constantine latitude, because it permits to receive the maximum annual energy.

The bottom losses coefficient is approximately [20]:

$$U_{bot} = \frac{K_{in}}{\varepsilon_{in}} \tag{11}$$

For the TIM cover, we have used the experimental results which can be expressed as a linear function of temperature difference [21]:

$$U_{top} = \left[1.14 + 0.11\left(T_w - T_{amb}\right)\right]$$

The set of equations (1) to (8) with the initial and boundary conditions discussed above are not sufficient to solve the problem, we need to another condition to determine the pressure inside the adsorber, and this condition is described as follows:

During the isosteric heating and cooling processes, we have considered a constant mean concentration and with the assumption that the pressure is uniform, we can obtain the pressure time variation as [18]:

$$\frac{d\ln p}{dt} = \frac{\iint b \frac{q_{st}}{R T^2} \frac{dT}{dt} r\, dr\, dz}{\iint b\, r\, dr\, dz} \tag{12}$$

When the condensation and evaporation takes place, we assume that the pressure inside the adsorber becomes equal to saturation pressure at condensation or evaporation temperature, respectively.

4. METHOD OF RESOLUTION

The foregoing model requires the simultaneous solution of a set of partial differential and algebraic equations. These equations are discretized by using a fully implicit finite difference method in order to obtain four unknowns: the adsorber wall temperature, the adsorbent temperature (Activated carbon), the pressure (methanol) and the adsorbed mass during a fully cycle.

We note that the matrix associated with system's equation is a full matrix in the isosteric periods and a tridiagonal in the isobaric periods because of the absence of term of pressure in the equation (4) following the last assumption of the model.

5. SOLAR PERFORMANCE COEFFICIENT

The solar performance coefficient COP_s defined as the ratio of the cooling power to the incident global irradiance during the whole day:

$$COP_s = \frac{Q_f}{G_{tot}} \tag{13}$$

Q_f is the cooling power is produced at evaporator level, which can be written as:

$$Q_f = m_a \int_{t_{c/2}}^{t_c} \left(L(T_e) - \int_{T_e}^{T_c} C_{pl}(T)\, dT \right) \frac{dm}{dt} \approx m_a\, \Delta m \left[L(T_e) - C_{pl}(T_c - T_e) \right] \tag{14}$$

where, the amount of adorbate circulating in the system Δm, should be known and it is defined as the difference between total adsorbed mass during the heating isoster and the total adsorbed mass during cooling isoster (Fig. 2), calculated as:

$$\Delta m = m_{max} - m_{min} = m(T_a, P_e) - m(T_g, P_c) \tag{15}$$

where m_{max} is the adsorbed mass correspondent to the adsorption temperature T_a and evaporation pressure P_e; m_{min} is the adsorbed mass correspondent to the regenerating temperature T_g and condensation pressure P_c.

G_{tot} is the total solar energy absorbed by the collector during the whole day, which can be calculated by:

$$G_{tot} = \int_{sunrise}^{sunset} G(t)\, dt \tag{16}$$

6. RESULTS AND DISCUSSION

A computer program was done on the basis of the numerical methodology mentioned above to solve the model. Some basic parameters used in the model are listed in **Table 1**.

To validate the model, a thermodynamic cycle presented in Clapeyron diagram (pressure-overage temperature) is calculated and compared with ideal one. As can bee seen from the figure 5, the agreement is good, except a small discrepancy is noticed in the limit points of adsorption and desorption. So, this comparison shows that the developed model can described the behaviour and the effect of the thermal processes in the actual adsorber of a solar refrigerator. The effect of some parameters on the solar performance coefficient and cooling power will be discussed in the following sections.

Table 1: Parameters values and operating conditions used in the model

Name	Symbole	Value	Unit
Dubinin parameters	D	$5.02\ 10^{-7}$	
	n	2.15	
Maximum adsorption capacity	w_0	$0.425\ 10^{-3}$	m^3/kg
Ambient temperature	T_{amb}	25	°C
Adsorption temperature	T_a	25	°C
Condensation temperature	T_c	30	°C
Evaporation temperature	T_e	-5	°C
Specific heat of the adsorbent	C_{p2}	920	J/kgK
Specific heat of the metal of the adsorber	C_w	380	J/kgK
Metal density of the adsorber	ρ_w	7800	kg/m^3
Equivalent conductivity of the solid adsorbent	k	0.19	W/mK
Heat transfer coefficient	h	16.5	W/m^2K
Metallic net radius of the adsorber	R_1	0.016	m
Internal adsorber radius	R_2	0.038	m
External adsorber radius	R_3	0.040	m
Total solar energy	G_{tot}	26.12	MJ/m^2
Glass cover transmissivity	τ_v	0.9	
Absorption coefficient of the adsorber wall	α_w	0.8	
Adsorber length	L_t	1	m
Emissivity of the adsorber wall	ε_w	0.1	
Emissivity of the glass cover	ε_g	0.88	
Wind velocity	V	1	m/s
Mass of the adsorbent	m_a	21	kg
The heat losses coefficient at the bottom	U_{bot}	0.9	W/m^2K

6.1 Effect of condensation temperature

Figure 6 shows the effect of condensation temperature on the system performance. It can be seen that both solar performance coefficient COP_s and cooling power Q_f decrease almost linearly with increasing condensation temperature over the range shown, because of an increase in condensation temperature makes the saturation pressure $P_s(T_c)$ increases, so, the adsorbed mass of the methanol $m(T_g, P_s(T_c))$ increases. Consequently, there is a decrease in the cycled mass of the methanol given by the equation (15), in the cooling power and, also, in the COP_s .

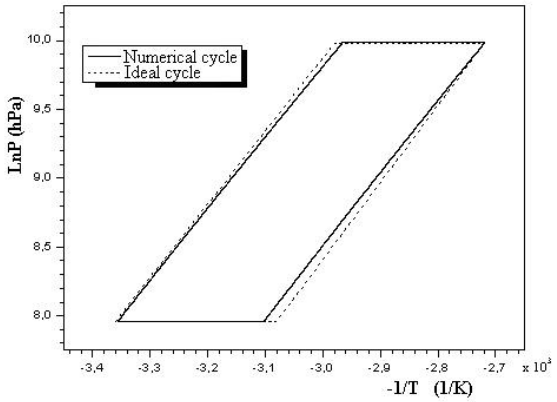

Fig. 5: Comparison between Numerical and ideal thermodynamic cycle

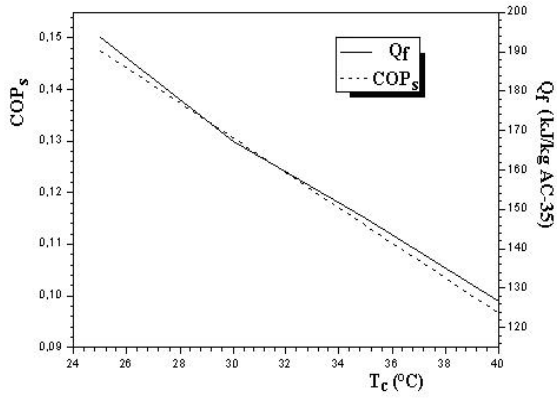

Fig. 6: The effect of condensation temperature T_c ($T_a = 25\,°C$, $T_e = -5\,°C$)

These results can be predicted directly from the Clapeyron diagram of adsorption cycle (Fig.2). It can be seen that the cycled mass $\left(m_{max} - m_{min}\right)$ decreases for a low condensation temperature with a fixed regenerating temperature T_g . Equation (14) shows that the cooling power Q_f is proportional to the cycled mass of methanol. Thus, an increase in T_c will result a reduction in the COP_s .

6.2 Effect of evaporation temperature

The effect of evaporation temperature T_e on system performance is shown in figure 7. As can be seen from this figure, both the COP_s and cooling power Q_f increases as evaporation temperature increases. This increment in evaporation temperature implies that the saturation pressure $P_s\left(T_e\right)$ increases together with the adsorbed mass of the methanol $m\left(T_a, P_s\left(T_e\right)\right)$. Therefore, it increases the cycled mass of the methanol given by the equation (15), the cooling power increases and, also, the COP_s . The Clapeyron diagram of adsorption cycle (Fig. 2) also shows that the cycled mass will increase as T_e is increased.

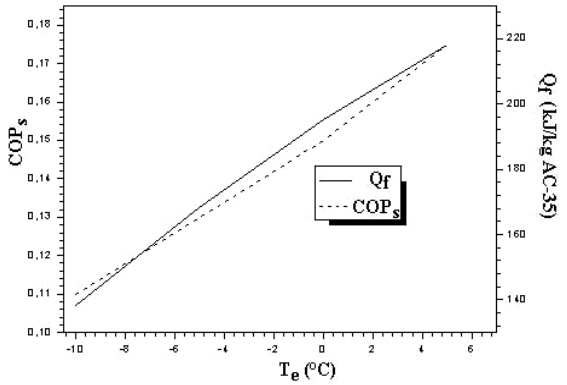

Fig. 7: The effect of evaporation temperature T_e (T_a = 25 °C , T_c = 30 °C)

Generally, T_e depends on the application goal, i.e. for the ice making it is better to limit it between -5 °C and: -10 °C and for air conditioning and vaccination storage T_e can be increased to around 5 °C and 8 °C, respectively. For solar adsorption refrigerator, because the energy of solar radiation is limited by weather condition, the evaporation temperature is in the range of $-10\,°C \le T_e \le 0\,°C$. If evaporation temperature above 0 °C , Zeolite / water pair can be used; this will cause a good refrigeration effect because the latent heat of water is larger than that of methanol.

6.3 Effect of adsorption temperature

Figure 8 shows the behaviour of the cooling power Q_f and the system's COP_s as function of the adsorption temperature. A similar effect observed for condensation temperature is noted for the adsorption temperature. The Clapeyron diagram (Fig. 2) shows that a decreasing in T_a increases the adsorbed mass $m(T_a , P_s(T_e))$ and the cycled mass, increasing the cooling power and the COP_s of the system. Generally, this temperature is mostly governed by the surrounding temperature, i. e. the ambient temperature. Consequently, the adsorption temperature should be as low as possible during the adsorption period. To achieve this condition, certain modifications were made in the collector, windows (airing shutters) were provided in the sides of the collector to open at night (adsorption process), and also flexible insulators are provided at the back of the collectors, which intensifies the nocturnal cooling.

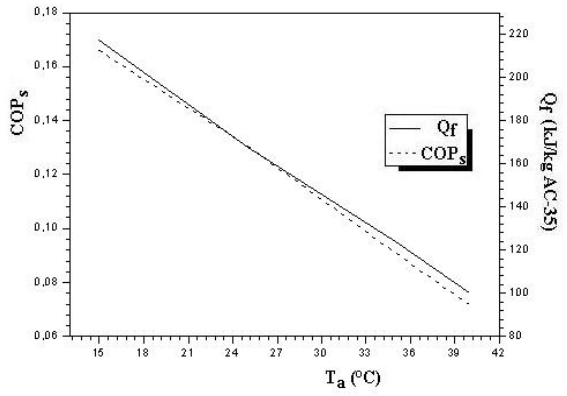

Fig. 8: The effect of adsorption temperature T_a ($T_e = -5\,°C$, T_c = 30 °C)

6.4 Effect of total solar energy

The solar refrigerator is powered by solar radiation energy, therefore the solar energy intensity decides the cooling power as well as the solar performance coefficient COP_s value, and these effects are shown in figure 9. We can see that both of cooling power Q_f and solar performance coefficient COP_s increase with the increase of the total solar energy absorbed by the collector.

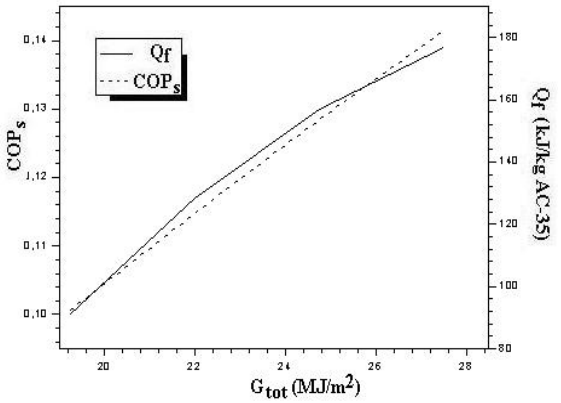

Fig. 9: The effect of the total solar energy absorbed by the collector
($T_a = 25\,°C$, $T_e = -5\,°C$ and $T_c = 30\,°C$)

However, there is a minimum value of solar radiation intensity under which no ice can be produced in practical application, because the amount of desorbed methanol, when evaporated, is just assured for providing cooling to evaporator. This minimum value of solar intensity depends on the variations of the atmospheric temperature during the day and characteristics of solar refrigerator device, this minimum value is about 11 MJ/m^2 from the report of M. Pons *et al.* [22].

6.5 Effect of collector configuration

The collector configuration is one of the important parameters that affect the solar performance coefficient and cooling power of solar refrigerator.

Usually, the increase of glazing cover number is limited by collector structure and dimension; in common practice, not more than two or three glazings. **Table 2** shows the effects on the solar performance coefficient and cooling power when single glass cover, double glass cover and TIM cover are used, respectively. We can see that both of performance and cooling power are increased when the double glass cover or TIM cover are used; this result is due to that the heat losses with the TIM cover is lower than those related to a single glass cover and double glass cover as it is shown in figure 10. These results are the similar to a theoretical comparative study between TIM cover and single glass cover by Leite *et al.* [23], between double glass cover and single glass cover by M Li *et al.* [24], and experimentally study reported by R.E. Critoph *et al.* [25], between a three kinds of the collector configuration.

Table 2: The effect of the collector configuration on the COP_s and Q_f .

Collector configuration	Q_f (kJ / kg AC − 35)	COP_s
Single glazed	168.192	0.13
Double glazed	213.661	0.172
TIM cover	229.286	0.184

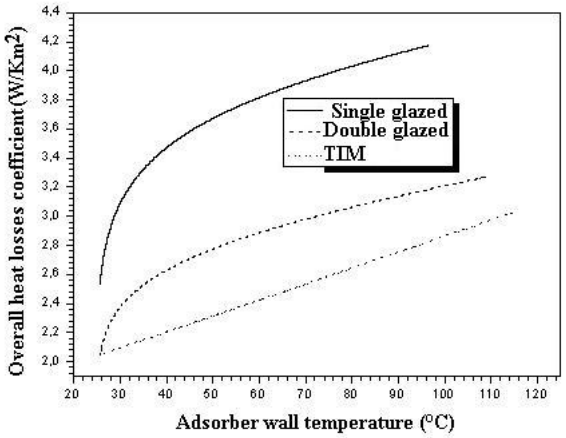

Fig. 10: The effect of the collector configuration on the overall heat losses coefficient ($T_a = 25\,°C$, $T_e = -5\,°C$ and $T_c = 30\,°C$)

7. CONCLUSION

A parametric study of the system performance of a combined heat and mass adsorption cooling system based on the Activated carbon A-C35/ methanol pair was carried out using a one dimensional numerical model, which is based on the behaviour of adsorber component and idealizing of the condenser and evaporator components. The numerical simulations have shown that:

- The refrigerator's increasing performance was mainly due to the result obtained from adsorptive refrigerator with a TIM or double glass cover.
- The cooling power Q_f and solar performance coefficient COP_s increase with increasing the evaporation temperature and decrease with the increase of the adsorption and condensation temperatures.
- The cooling power Q_f and solar performance coefficient COP_s increase with the increase of the total solar energy absorbed by the collector.

NOMENCLATURE

T	: Temperature, °C	T_a	: Adsorption temperature, °C
P	: Pressure, Pa	T_{c1}	: Limit temperature of desorption, °C
m	: Adsorbed mass, kg/kg	T_{c2}	: Limit temperature of adsorption, °C
w_0	: Maximum adsorption capacity m^3/kg	T_g	: Regenerating temperature, °C
D, n	: Characteristic parameters of adsorbent/adsorbate pair	T_c	: Condensation temperature, °C
$P_s(T)$	: Saturation pressure of the adsorbate, Pa	T_e	: Evaporation temperature, °C
q_{st}	: Isosteric heat of adsorption, kJ/kg	T_w	: Metallic wall temperature of the adsorber, °C
L	: Latent heat of evaporation, kJ/kg	T_{amb}	: Ambient temperature, °C
R	: Universal gas constant, J/kg K	m_{max}	: Adsorption mass at adsorbed state, kg/kg

P_e	: Evaporation pressure, Pa	m_{min}	: Adsorption mass at desorbed state, kg/kg
P_c	: Condensation pressure, Pa	Δm	: Cycled mass of the adsorbate, kg/kg
C_{pl}	: Specific heat of the adsorbate in liquid state, J/kg K	α	: Thermal expansion coefficient of the liquid adsorbate
C_{p2}	: Specific heat of the adsorbent, J/kg K	ρ_w	: Density of the metal of the adsorber, kg/m^3
C_w	: Specific heat of the metal of the adsorber, J/kg K	$\rho_l(T)$	: Density of the adsorbate, kg/m^3
k	: Equivalent conductivity of the solid adsorbent, W/m K	ε_{in}	: Thickness of the insulator, m
k_{in}	: Conductivity of the insulator, W/m K	V_w	: Volume of the adsorber, m^3
h	: Heat transfer coefficient between the tube wall and the adsorbent, W/m^{2}K	R_1	: Radius of the metallic net of the adsorber, m
R_2 , D_2	: Internal adsorber radius, diameter, m	R_3 , D_3	: External adsorber radius, diameter, m
$G(t)$	: Diurnal solar radiation, W/m^2	τ_v	: Glass cover transmissivity
G_{tot}	: Total solar radiation, W/m^2	α_w	: Absorption coefficient of the adsorber wall
U_L	: Overall heat losses coefficient, W/m^2 K	ε_w	: Emissivity of the adsorber wall
L_t	: Adsorber length, m	ε_g	: Emissivity of the glass cover
N_v	: Number of glass cover	V	: Wind velocity, m/s
h_v	: Wind heat transfer coefficient, W/m^{2}K	β	: Collector inclination, °
m_a	: Mass of the adsorbent, kg	σ	: Stefan-Botzman constant, W/m^{2}K^4
r	: Layer radius, m	$t_{c/2}$	: First half cycle time, s
t	: Time, s	Q_f	: Cooling power, KJ
t_c	: Cycle time, s	COP_s	: Solar performance coefficient

REFERENCES

[1] E. Passos, F. Meunier and G.C. Gianola, '*Thermodynamic Performance Improvement of an Intermittent Solar-Powered Refrigeration Cycle Using Adsorption of Methanol on Activated Carbon*', J. Heat Recovery Systems, Vol. 6, N°3, pp. 259 – 264, 1986.

[2] R.E. Critoph, '*Activated Carbon Adsorption Cycles for Refrigeration and Heat Pumping*', Carbon, Vol. 27, N°1, pp. 63 – 70, 1989.

[3] R.E. Critoph, '*Performance Limitations of Adsorption Cycles for Solar Cooling*', Solar Energy, Vol. 41, N°1, pp. 21 – 31, 1998.

[4] H. Jing and R.B.H. Exell, '*Adsorptive Properties of Activated Charcoal / Methanol Combination*', Renewable Energy, Vol. 3, N°6-7, pp. 567 – 675, 1993.

[5] R.E. Critoph, '*Evaluation of Alternative Refrigerant - Adsorbent Pairs for Refrigeration Cycles*', Applied Thermal Engineering, Vol. 16, N°11, pp. 891 – 900, 1996.

[6] N. Medini, B. Marmottant, E.S. Golli and P. Grenier, '*Study of a Solar Icemaker Machine*', Int. J. Refrig., Vol. 14, N°3, pp. 363 – 377, 1991.

[7] A. Boubakri, M. Arsalane, B. Yous, L. Alimoussa, M. Pons, F. Meunier and J.J. Guilleminot', '*Experimental Study of Adsorptive Solar Powered Ice Makers in Agadir (Morocco) – 1-Performance in Actual Site*', Renewable Energy, Vol. 2, N°1, pp. 7 – 13, 1992.

[8] A. Boubakri, M. Arsalane, B. Yous, L. Alimoussa, M. Pons, F. Meunier and J.J. Guilleminot', '*Meteorological Parameters*', Renewable Energy, Vol. 2, N°1, pp. 15 - 21, 1992.

[9] K. Sumathy and L. Zhongfu, '*Experiments with Solar-Powered Adsorption Ice- Maker*', Renewable Energy, Vol.16, pp. 704 – 707, 1999.

[10] F. Poyelle, J.J. Guilleminot and F. Meunier, '*Experimental Tests of and Pedictive Model of an Adsorptive Air Conditioning Unit*', Ind. Eng. Chem. Res. Vo. 38, pp. 298 – 309, 1999.

[11] A. Boubakri, J.J. Guilleminot and F. Meunier, '*Adsorptive Solar Powered Ice Maker: Experiments and Model*', Solar Energy, Vol. 69, N°3, pp. 249 - 363, 2000.

[12] A. Boubakri, '*A New Conception of an Adsorptive Solar-Powered Ice Maker*', Renewable Energy, Vol. 28, N°5, pp. 831 – 342, 2003.

[13] F. Buchter, P. Dind and M. Pons, '*An Experimental Solar-Powered Adsorptive Refrigerator Tested in Burkina-Faso*', Int. J. Refrig., Vol. 26, pp. 26 - 86, 2003.

[14] M. Li, H.B. Huang, R.Z. Wang, L.L. Wang, W.D. Cai and W.M. Yang, '*Experimental Study on Adsorbent of Activated Carbon with Refrigerant of Methanol and Ethanol for Ice Maker*', Renewable Energy, Vol. 29, N°15, pp. 2235 – 2244, 2004.

[15] C. Hildbrand, P. Dind, M. Pons and F. Buchter, '*A New Solar Powered Adsorption Refrigerator with High Performance*', Solar Energy, Vol. 77, N° 3, pp. 311 – 318, 2004.

[16] F. Lemmini and A. Errougani, '*Building and Experimentation of a Solar Powered Adsorption Refrigerator*', Renewable Energy, Vol. 30, N°13, pp. 1989 – 2003, 2005.

[17] A.P.F. Leite, M.B Grilo, R.R.D. Andrade, F.A. Belo and F. Meunier, '*Experimental Thermodynamic Cycles and Performance Analysis of a Solar - Powered Adsorptive Icemaker in Hot Humid Climate*', Renewable Energy, Article in Press.

[18] A.P.F. Leite and M. Daguenet, '*Performance of a New Solid Adsorption Ice Maker with Solar Energy Regeneration*', Energy Conversion and Management, Vol. 41, N°15, pp. 1625 – 1647, 2000.

[19] J.A. Duffie and W. Beckman, '*Solar Energy Thermal Processes*', John Wiley& Sons, Inc., 1974.

[20] E.E. Anyanwu, U.U. Oteh and N.V. Ogueke, '*Simulation of a Solid Adsorption Refrigerator Using Activated Carbon - Methanol Pair*', Energy Conversion and Management, Vol. 42, pp. 899 – 915, 2001.

[21] M. Rommel and A. Wagner, '*Application of Transparent Insulation Materials in Improved Flat-Plate Collectors and Integrated Collector Storages*', Solar Energy, Vol. 49, N°5, pp. 371 – 380, 1992.

[22] M. Pons and P. Grenier, '*Experimental Data on a Solar Powered Icemaker Using Activated Carbon and Methanol Adsorption Pair*', Journal of Solar Energy Engineering, Transaction of the ASME., Vol. 109, p. 303, 1987.

[23] A.P.F. Leite, M.B. Grilo, F.A. Belo and R.R.D. Andrade, '*Dimensioning, Thermal Analysis and Experimental Heat Loss Coefficients of an Adsorptive Solar Ice Maker*', Renewable Energy, Vol. 29, pp. 1643 – 1663, 2004.

[24] M. Li and R.Z. Wang, '*A Study of the Effects of Collector and Environment Parameters on the Performance of a Solar Powered Solid Adsorption Refrigerator*', Renewable Energy, Vol. 27, pp. 369 - 382, 2002.

[25] R.E. Critoph and Z. Tamainnot-Teleto, '*Solar Sorption Refrigerator*', Renewable Energy, Vol. 12, N°4, pp. 409 – 417, 1997.